

Introduction to In Situ Forming Hydrogels for Biomedical Applications

**Bogyu Choi, Xian Jun Loh, Aloysius Tan, Chun Keat Loh, Enyi Ye,
Min Kyung Joo and Byeongmoon Jeong**

Abstract In situ gelling polymer aqueous solutions undergo sol-to-gel transition through chemical and/or physical crosslinking. The criterion on sol and gel is an important issue, therefore, rheology of hydrogel have been discussed in detail. The in situ gelling system has been investigated for minimally invasive drug delivery, injectable tissue engineering, gene delivery, and wound healing. In this chapter, in situ gelling systems and their various biomedical applications were briefly summarized.

Keywords Injectable · Rheology · Physical crosslinking · Thermogel · Tissue engineering

B. Choi

Division of Advanced Prosthodontics, University of California, Los Angeles,
CA 90095, USA

X.J. Loh (✉) · A. Tan · C.K. Loh · E. Ye

Institute of Materials Research and Engineering (IMRE), A*STAR, 3 Research Link,
Singapore 117602, Singapore
e-mail: lohxx@imre.a-star.edu.sg

X.J. Loh

Department of Materials Science and Engineering, National University of Singapore,
9 Engineering Drive 1, Singapore 117576, Singapore

X.J. Loh

Singapore Eye Research Institute, 11 Third Hospital Avenue, Singapore 168751, Singapore

M.K. Joo

Center for Theragnosis, Biomedical Research Institute, Korea Institute of Science
and Technology, Seoul, South Korea

B. Jeong (✉)

Department of Chemistry and Nano Science, Ewha Womans University,
52 Ewhayeodae-Gil, Seodaemun-Gu, Seoul 120-750, South Korea
e-mail: bjeong@ewha.ac.kr

1 Introduction

Hydrogels are hydrophilic macromolecular networks swollen in water or biological fluids [1]. Wichterle and Lim [2] reported the pioneering work using hydrophilic 2-hydroxyethyl methacrylate (HEMA) hydrogels in 1960. Recently, in situ gelling systems based on various natural and synthetic polymers have been widely investigated for biomedical applications due to effective encapsulation of cells and bioactive molecules, minimally invasive injection, and easy formation in any desired shape of defects, in addition to several advantages of typical hydrogels including high water contents similar to extracellular matrix (ECM), controllable physicochemical properties, and efficient mass transfer [3–5]. When hydrogels are prepared by covalent-crosslinking, they form permanent or chemical gels. On the other hand, when physical intermolecular association induces hydrogels, the hydrogels form physical gels and their formations are usually reversible.

2 Chemical Hydrogels

Chemical hydrogels are 3D crosslinked networks that formed by new covalent bonds between water-soluble macromers. To use chemical hydrogels for biomedical application, chemical reactions should not damage incorporated biopharmaceuticals or cells. There are several chemical crosslinking methods such as redox-initiated polymerization, photopolymerization, classical organic reactions between functional groups, and enzymatic reactions.

Redox-initiated polymerization using ammonium persulfate (APS)/N,N,N',N'-tetramethylethylenediamine (TEMED) or APS/ascorbic acid has been used to encapsulate cells in poly(ethylene glycol) (PEG), oligo(PEG fumarate) (OPF), poly(lactide-co-ethylene oxide-co-fumarate) (PLEOF), chitosan derivatives, or carboxybetaine hydrogels [6–11]. In these systems, an increase of initiator concentration led a decrease in the gelling time, however, it also affected the cell viability. Therefore, low cytotoxic free radical polymerization is needed to use this method for biomedical applications.

Photo polymerization of vinyl groups bearing polymers via ultraviolet (UV) or visible light irradiation with photoinitiators is one of most common and effective encapsulation methods for cell or bioactive molecules in biomedical applications. The hydrogel can be performed at physiological pH and temperature. Various photo initiators, such as 2-hydroxy-1-[4-(hydroxyethoxy)phenyl]-2-methyl 1-propanone (Irgacure 2959) [12–14], lithium acyl phosphinate (LAP) [15, 16], methyl benzoylformate (MBF) [17], or 2,2-dimethoxy-2-phenylacetophenone (DMPA) [18] have been used to produce UV sensitive hydrogels. UV-initiated free radical polymerization systems showed lower cytotoxicity than redox-initiated polymerization. However, UV-irradiation can damage cells, proteins, or tissues; therefore, visible light inducible hydrogel systems have been developed. Exposure to

visible light is less-thermogenic yet causes less cell damage. In addition, visible light penetrating through human skin provided greater depth of cure than UV [19]. Riboflavin (vitamin B2) [20], eosin-Y [21, 22], or ruthenium (Ru (II))/sodium persulphate (SPS) [23] have been used as a visible light initiator.

Crosslinking via reactions between functional groups present in the water-soluble monomers or macromers produce hydrogels. Classical organic reactions between functional groups such as the Michael addition, click reaction, Schiff base formation, epoxide coupling, genipin coupling, and disulfide exchange reaction have been used to prepare hydrogels. The Michael addition of nucleophiles (amine or thiol group) to α,β -unsaturated carbonyl compounds or α,β -unsaturated sulfones in water forms hydrogels. Various functionalized polymers, such as poly(ethylene glycol) (PEG) [24–26], poly(vinyl alcohol) (PVA) [27], N-isopropylacrylamide (NIPAAm) [28], and natural polymers [14, 29] have been crosslinked via Michael addition and formed hydrogels. The copper [Cu(I)] catalyzed azide-alkyne cycloaddition is one of the most popular click chemistry reactions. Macromolecular derivatives of PVA [30], PEG [31–33], NIPAAm [34], and polysaccharides [35] with Cu(I) as a catalyst have been used to prepare in situ forming hydrogels. However, cytotoxic problem of Cu(I) should be solved to use these click chemistry induced hydrogels for biomedical applications. Thus, Cu(I)-free click reactions have been developed to be used as a tissue engineering scaffolds [36, 37]. The Diels-Alder reaction, highly selective [4 + 2] cycloaddition between a diene and a dienophile without a catalyst, is also known as a click type reaction. Diels-Alder click crosslinked PEG [38], NIPAAm [39], or hyaluronic acid (HA) [40, 41] based hydrogels have been investigated for tissue engineering applications.¹

There has been an increased interest in the enzymatically crosslinked hydrogels that shows few side reactions since their high specificity for substrates. Horseradish peroxidase (HRP)/hydrogen peroxide (H_2O_2), transglutaminase (TG), phosphatase (PP), tyrosinase, or thermolysin catalyzed crosslinking provides in situ hydrogel formation of hydroxyphenyl propionic acid (HPA) functionalized 8-arm PEG [42], thiol functionalized poly(glycidol) [43], Tetronic-tyramine (Tet-TA)/gelatin-HPA (GFPA) [44], dextran-tyramine (Dex-TA) [45], alginate-g-pyrrole [46], or protein polymers containing either lysine or glutamine [47]. These enzymatic crosslinks provide fast gelation.

3 Physical Hydrogels

Heat, ions, inclusion complex, stereocomplex, and/or complimentary binding can induce a hydrogel formation by forming physical junctions via molecular entanglement, crystalline order, or intermolecular interactions. Hydrogels formed by physical association are called physical, reversible, and stimuli responsive hydrogels. These hydrogel systems should be biocompatible with a host as well as the incorporated bioactive agents.

Polymers containing well balanced hydrophilic blocks and hydrophobic blocks can physically crosslink as temperature increases by forming associations of hydrophobic domains. PEG has been used as a hydrophilic block in most of the thermogelling systems. Thermogelling systems that show sol-to-gel transition at around physiological temperature have been widely developed for injectable biomedical applications. At low temperature, thermo-sensitive polymer aqueous solution is easy to mix with cells, drugs, and/or bioactive molecules, followed by an injection of the mixture to target site to form a hydrogel. The target site can be a subcutaneous layer for a protein drug delivery, a tumor tissue for an anticancer drug delivery, or a damaged defect for tissue regeneration. As thermogelling polymers, (1) polyacrylates: NIPAAm copolymers and mono and dilactate substitute poly(2-hydroxypropyl methacrylamide), (2) polyesters: PEG/PLGA, PEG/poly(ϵ -caprolactone) (PCL), and PEG/poly(ϵ -caprolactone-co-lactide) (PCLA) block copolymers, (3) poly(ester urethane) (poly(1,4-butylene adipate) (PBA)/PEG/PPG connected by hexamethylene diisocyanate, (4) natural polymer and its derivatives (chitosan/ β -glycerol phosphate, chitosan-g-PEG, HA-g-PNIPAAm, (5) polyphosphazenes, (6) Pluronic[®] and its derivatives, (7) poly(trimethylene carbonate), and (8) polypeptides: elastin-like (VPGVG) polypeptide (ELP), silk-like (GAGAGS) polypeptides, polyalanine (PA), poly(alanine-co-phenylalanine) (PAF), poly(alanine-co-leucine) (PAL), etc. have been developed [48–61]. Polypeptide-based thermogelling systems have several advantages compared with polyester-based hydrogels. (1) During gel degradation, polypeptide thermogels maintain neutral pH since degradation products are neutral amino acids, while pH of polyester thermogels decreases due to their acidic degradation products. Decrease in pH can be a problem for biomedical applications, since it can decrease cell viability or protein drug stability. (2) Enzyme-sensitive degradation of the polypeptide-based hydrogel systems provides a storage stability of the encapsulated material in vitro [62]. (3) Polypeptides have unique secondary structures including α -helix, β -sheet, triple helix, and random coil, allowing various nano-assemblies followed by sol-to-gel transition. These nano-assemblies can give unique nanostructures in the hydrogels. Thus, polypeptide-based hydrogels can provide biomimetic ECMs with various nanostructures that can affect proliferation and/or differentiation of encapsulated cells [3, 63].

Crosslinking by addition of ions provides reversible hydrogels. Alginate hydrogel formation using calcium ions can be carried out at mild condition of room temperature and physiological pH. Therefore, alginate gels have been used for encapsulating cells and protein drugs [64]. Salts in media also triggered MAX8 (VKVKVKVKV^DP^L-PTKVEVKVKV-NH₂) and HLT2 (VLTKVKTKV^DP^L-PTKVEVKVLV-NH₂) peptides to fold into a β -hairpin conformation that induced hydrogel formation [65].

Inclusion complexes between cyclodextrins (CDs) and guest molecules induce physical associations to form physical hydrogels. There are three subtypes of α -, β -, γ -CDs consisting of 6, 7, and 8 glucopyranose units, where the internal diameter of the cavity are 5.7, 7.8, and 9.5 Å, respectively [66]. Different-sized guest molecules can selectively insert into the inner cavity of CD with proper diameter.

Sequential inclusion complexations were used to form an in situ hydrogel [67]. First, Pluronic[®]s were immobilized on the cellulose nanocrystal via interaction between PPG block of Pluronic[®] and β -CD on the nanocrystal surface, and then uncovered PEG blocks of Pluronic[®] were inserted into cavity of α -CD followed by in situ hydrogel formation.

Stereocomplexation between enantiomers by stereoselective van der Waals interaction have been used in the design of in situ hydrogel systems. Mixing two polymer aqueous solutions containing poly(L-lactide) (PLLA) block and poly(D-lactide) (PDLA) block induces a stereocomplexed hydrogel. Stereocomplex of PLLA-PEG-PLLA, PDLA-b-cationic poly(carbonate)-PDLA (PDLA-CPC-PDLA), and PDLA-PEG-PDLA triblock copolymers provided a thermosensitive antimicrobial hydrogel [68]. The 8-armed star block copolymers of PEG-(NHCO)-(PDLA)₈ and PEG-(NHCO)-(PLLA)₈ were mixed to form stereocomplexed spontaneous hydrogel [69].

Complementary binding such as antigen/antibody interactions, ligand/receptor interactions, and base-pairing interactions between oligonucleotides can also form in situ hydrogels. Acrylamides attached either an antigen (rabbit immunoglobulin G; rabbit IgG) or its specific antibody (goat anti-rabbit IgG) formed semi-interpenetrating network hydrogel [70]. Gyrase subunit B (GyrB) was dimerized by the addition of the aminocoumarin antibiotic coumermycin, resulting in hydrogel formation [71]. Addition of increasing concentrations of clinically validated novobiocin (Albamycin) dissociated the GyrB subunits, thereby resulting in gel-to-sol transition. Multi-arm star shaped PEG functionalized with thymine and adenine self-assembled via base pairing of thymine and adenine to form a hydrogel [72]. The potential of this biological hydrogel for targeted growth factor delivery and cell encapsulation was confirmed.

4 Combining Chemical and Physical Crosslinking

Generally, physical hydrogels have the limitation of weak mechanical properties, thus, a combination of chemical and physical crosslinking has been used to overcome this weakness. Thiolated chondroitin sulfate (CS-TGA)/PEG diacrylate (PEGDA)/ β -glycerophosphate disodium salt (β -GP) mixture formed hydrogel by Michael addition, disulfide bond forming, and temperature increasing to 37 °C [73]. The PNIPAAm-co-glycidyl methacrylate (GMA)/polyamidoamine (PAMAM) mixed solution was formed hydrogel by a physical and chemical dual-gelation [74].

5 Hydrogel Rheology

The basic principles and different aspects of hydrogels have been covered in several reviews [4, 75–77]. The mechanical properties of a hydrogel are important considerations for specific biological applications [78]. The free-standing ability

of the gel is an important consideration for cell growth scaffolds. The stiffness of hydrogels has been reported to direct the differentiation of different cell types [79–81]. For drug delivery, hydrogels should preferentially reduce in viscosity upon injection and undergo rapid recovery upon removal of the stress to form the drug release gel depot. This design principle has been the basis of several in situ thermogelling polymeric networks [5, 82–84]. Finally, rheological measurements allow for the understanding of the different gelation mechanisms which can be utilized in the optimization of the properties of the hydrogels for tissue reconstruction and drug delivery applications.

The flow and strain properties of soft materials have been extensively investigated since the 17th century. In the 1830s, scientists discovered that many materials possess time-dependent mechanical properties under various conditions, which cannot be explained by the classical theory of Newtonian fluid. For example, in 1835, Weber observed the phenomenon of elastic hysteresis when he studied the uranium filament. In 1865, Lord Kelvin discovered the viscosity behavior of zinc, and that its inner impedance was not proportional to the strain rate. Two years later, Maxwell proposed a model for viscoelastic materials having properties both of viscosity and elasticity. The Maxwell model can be simply represented by the series connection of a purely elastic spring and a purely viscous damper. At the same time, scientists also found many fluids, which were all called non-Newtonian fluid later due to the nonlinear relationship between the shear stress and shear rate. Based on the known constitutive equation, people proposed the concept of stress relaxation time, suggesting the viscosity to be the product of the elastic modulus and the stress relaxation time. In 1874, Boltzmann developed the linear viscoelasticity theory, suggesting that the stress in a given time is not only related to the strain in the given time, but also dependent on its previous deformation. In 1940s, Reiner pointed out that in order to eliminate the Weissenberg effect (The Weissenberg effect is a phenomenon that occurs when a spinning rod is inserted into a solution of liquid polymer. Instead of being thrown outward, the solution is drawn towards the rod and rises up around it), a stress proportional to the square of the spinning speed needs to be applied [85]. Almost at the same time, Rivlin's study on the torsion of a rubber cylinder helped to solve the problem of Poynting effect [86]. The intrinsic significance of these two studies is to further apply the generalized approach regarding the nonlinear constitutive equation, which brought in flourishing progress in the field of rheology. With the advance in rational mechanics, from small deformation theory to finite deformation theory, from linear theory to nonlinear constitutive theory, from classical object model to microstructure theory, rheology rapidly advanced after 1965, moving from phenomenological theory, which describes phenomena only into the ontology, which considers the internal structure. The term "rheology" was first coined by Bingham and Reiner in 1929 when the American Society of Rheology was founded in Columbus, Ohio [87]. This term was inspired by a Greek quotation, "panta rei", "everything flows". In the same year, Journal of Rheology started its publication. In 1932, the Committee on Viscosity of the Academy of Sciences at Amsterdam was founded, which was later renamed The Dutch Rheological Society in 1951. The British Society of Rheology was founded

as an informal British Rheologists' Club in 1940. In the following years, Society of Rheology/Group of Rheology was founded in countries like Germany, Austria, Belgium, Sweden, Czech Republic, France, Italy, Israel, Japan and Australia. Many of these societies/groups became members of the European Society of Rheology later, greatly promoting the development of rheology. Basically, rheology is defined as the science of the deformation and flow of matter, thus it mainly focuses on the investigation of the time-dependent strain and flow properties of soft materials under conditions like stress, strain, temperature, humidity and radiation [88]. Rheological parameters include the physic-mechanical properties of liquids and solids which describe strain and flow behavior. When external forces are exerted on the materials, strain can be measured and experimentally studied.

The viscoelastic properties of hydrogels can be determined by rheometry. The basics and theories of rheology, its measurements and the types of equipment can be found in several seminal publications [89, 90].

In rheology, the variable shear stress, τ , is defined as the ratio of the force F applied on a sample area A to cause the disruption of the material between the two plates. The strain, γ , is defined as the ratio of the deviation of x of the sample to the height of the sample, h or more simply defined as $\tan \alpha$. The velocity of the movement at the applied force is controlled by the internal force acting within the material.

The mechanical properties of hydrogels are determined by small perturbation rheology experiments on hydrogels. When the hydrogel is subjected to a small perturbation, the material particles are displaced relative to each other resulting in strain. When external anisotropic forces are exerted on elastic bodies, they undergo elastic strain. A spontaneous full recovery of the original form of the material results when the external force is removed. On the contrary, the strain on viscous bodies is irreversible once external anisotropic forces are exerted. The input energy is transformed and this causes the material to flow. Hydrogel materials are neither completely viscous nor elastic; instead it exhibits a behavior known as viscoelasticity. These small perturbations of the hydrogels are meant to ensure that the rheology experiment is carried out within the linear viscoelastic region (LVR) of the material, hence ensuring the measured properties of the hydrogels are independent of the magnitude of imposed strain or stress. In addition, the linear viscoelasticity region is when the magnitude and stress are related linearly. When small deformation is applied sufficiently slowly, the molecular arrangements of the polymers are still close to equilibrium. The mechanical response is then just a reflection of dynamic processes at the molecular level, which go on constantly, even for a system at equilibrium (Fig. 1).

Small amplitude oscillatory shear measurements, creep and creep recovery tests are examples of small perturbation tests carried out on hydrogels. The principle of small amplitude oscillatory shear measurements is shown in Fig. 2.

By applying shear stress, a laminar shear flow is generated between the two plates. The uppermost layer moves at the maximum velocity V_{\max} , while the lowermost layer remains at rest. The shear rates of typical actions are summarized in Table 1.

$$\text{Shear rate } \dot{\gamma} = \frac{dv}{dh}$$

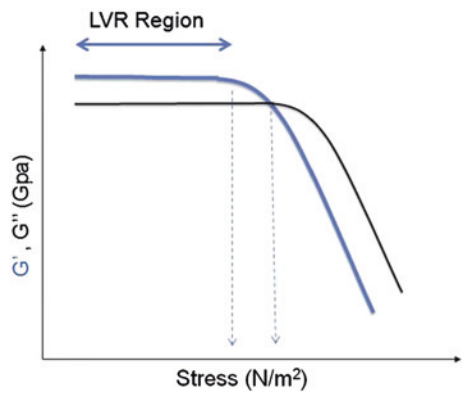


Fig. 1 Illustration of the linear viscoelastic region (LVR)

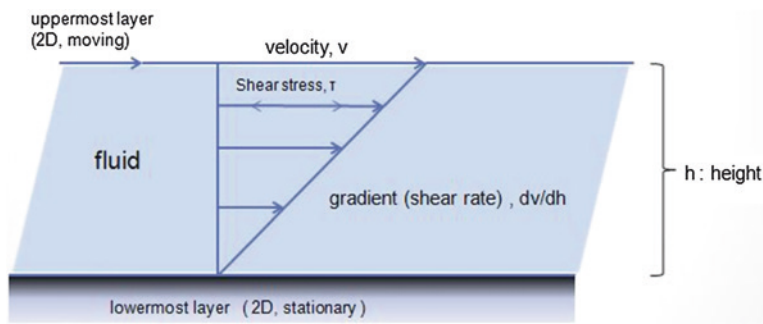
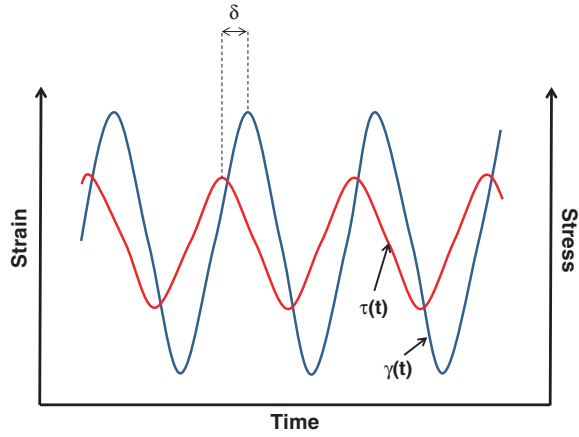


Fig. 2 Shear forces in rheology

Table 1 Examples of actions and the shear rate involved

Actions	Shear rate/s ⁻¹
Spraying	10 ⁴ –10 ⁵
Rubbing	10 ⁴ –10 ⁵
Curtain coating	10 ² –10 ³
Mixing	10 ¹ –10 ³
Stirring	10 ¹ –10 ³
Brushing	10 ¹ –10 ²
Chewing	10 ¹ –10 ²
Pumping	10 ⁰ –10 ³
Extruding	10 ⁰ –10 ²
Levelling	10 ⁻¹ –10 ⁻²
Sagging	10 ⁻¹ –10 ⁻²
Sedimentation	10 ⁻¹ –10 ⁻³

Fig. 3 Principle of a small amplitude oscillatory shear measurement

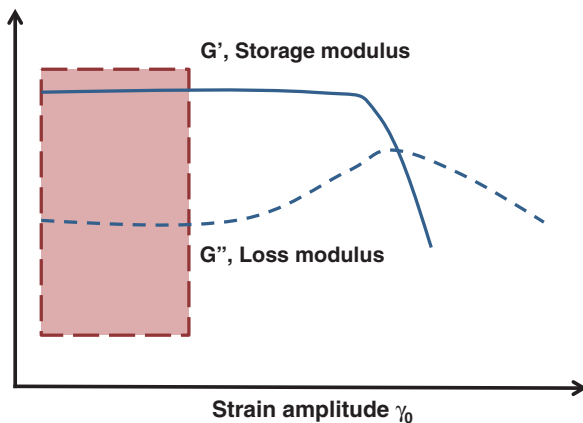


For controlled-strain rheometers, the shear strain that is a sinusoidal function of time, t , can be expressed as, $\gamma(t) = \gamma_0(\sin \omega t)$, where γ_0 is the amplitude of the applied strain and ω is the angular frequency of oscillation (in rad s^{-1}). The angular frequency is related to frequency, f , measured in cycles per second (Hz) whereby $\omega = 2\pi f$. The shear stress resulting from the applied sinusoidal strain will also be a sinusoidal function, which can be expressed as $\tau(t) = \tau_0(\sin \omega t + \delta)$ in which τ_0 is the amplitude of the stress response and δ is the phase difference between the two waves.

On the other hand, for stress-controlled rheometers, the shear stress is applied as $\tau(t) = \tau_0(\sin \omega t)$ and the resulting shear strain is measured as $\gamma(t) = \gamma_0(\sin \omega t + \delta)$. For a purely elastic material, it follows from Hooke's law that the strain and stress waves are always in phase ($\delta = 0^\circ$). On the other hand, while a purely viscous response has the two waves out of phase by 90° ($\delta = 90^\circ$). Viscoelastic materials give rise to a phase-angle somewhere in between (Fig. 3).

In small amplitude oscillatory shear measurements, the shear storage modulus, G' , loss modulus, G'' , and loss factor, $\tan \delta$, are critical hydrogel properties monitored against time, frequency and strain. An alternative approach to discuss the dynamic response of a viscoelastic material is by using complex notation to describe an applied sinusoidal strain, $\gamma^* = \gamma_0 \exp(i\omega t)$, whereby $i = \sqrt{-1}$, the complex stress can be expressed as $\tau^* = \tau_0 \exp[i(\omega t + \delta)]$. From Hooke's law, the complex modulus of the tested material is $G^*(\omega) = \tau^*/\gamma^* = (\tau_0/\gamma_0) \exp(i\delta)$. This expression can be resolved into an in-phase component and an out-of-phase component by a substitution of the Euler's identity where $\exp(i\delta) = \cos \delta + i \sin \delta$. This gives $G^*(\omega) = G' + iG''$ with G' and G'' as the real (i.e. elastic or in phase) and imaginary (i.e. viscous or loss or out-of-phase) components of G^* , respectively. The loss factor, $\tan \delta$, is defined as G''/G' . To re-emphasize, G' measures the deformation energy stored during shear process of a test material which is characteristic of the stiffness of the material and G'' is representative of the energy dissipated during shear which is characteristic of the flow response of the

Fig. 4 Typical graph showing storage and loss modulus



material. If $\tan \delta > 1$ ($G'' > G'$), the sample behaves more like a viscous liquid while, conversely, when $\tan \delta < 1$ ($G' > G''$), the sample behaves more like an elastic solid (Fig. 4).

For gel samples, these parameters are often measured as a function of time, strain and frequency. Observation of the gelation process can be achieved by monitoring the temporal evolution of G' and G'' . The linear viscoelastic region within which G' and G'' are independent of shear strain can be determined by monitoring the moduli of the material as a function of the strain.

The behavior of the hydrogel at short and long timescales can be studied by measurement of the moduli of the material as a function of frequency. The frequency dependence of the moduli is a critical hydrogel parameter since a single material can look quite solid-like ($G' \gg G''$) at a high frequency (short timescale) but behave much more liquid-like ($G'' > G'$) at low frequency (long timescale). Gelation kinetics and final gel stiffness are critical material properties that directly impact the application of the material.

Besides small perturbation measurements, creep and creep recovery tests are also employed to investigate the time-dependent evolution of compliance. This aids in the critical understanding of the long-term viscoelastic behavior of hydrogels. Different mammalian cells exert different stress levels on the hydrogel scaffolds and they behave differently in response to the compliance of the gel material. In typical experimental setups, creep and creep recovery tests are performed consecutively. For this experiment, there is an instantaneous increase in the stress from 0 to τ_1 . This is kept constant from t_0 to t_1 in the creep phase to subject the material to a prolonged period of stress. Then the stress is completely removed in the subsequent recovery phase. The resulting strain is recorded as a function of time ($t_0 < t < t_2$) in both tests. The creep compliance is defined as $J(t) = \gamma(t)/\tau_0$ which has a unit of reciprocal modulus (Pa^{-1}). Within the linear viscoelastic region, the creep compliance is independent of applied stress and all $J(t)$ curves obtained under various stresses should overlap with each other. Sometimes creep

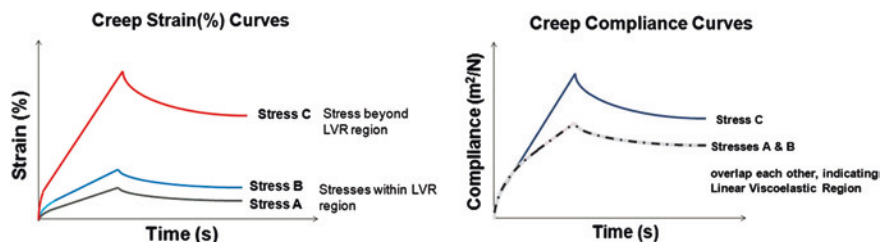


Fig. 5 Sample creep curves under different stresses

compliance is compared to reciprocal shear modulus measured in small amplitude oscillatory shear tests in order to judge if the sample displays pure elastic behavior. Figure 5 shows a typical example of creep strain curves and creep compliance curves of polystyrene at various stresses. In the linear viscoelasticity region, under different stresses of A and B, the creep compliance curves overlap each other. The curve induced by Stress C does not overlap as shown in Fig. 5, indicating that the linear viscoelasticity region has been exceeded.

In addition to the above-mentioned measurements, the flow properties of the hydrogels as well as their abilities to retain or recover their original form after experiencing shear flow or large strain are important factors to understand. Shear-thinning and self-healing hydrogels are excellent candidates for injectable therapeutic delivery vehicles. Monitoring rheological behavior and structural evolution of these gels during and after flow can help evaluate encapsulated therapy retention and delivery during syringe injection and the ability of the material to stay localized after injection against possible biological forces in vivo (Fig. 6).

Inspired by our bodies' ability to heal, self-healing materials have the ability to repair themselves when they are damaged. In the literature discussed in other chapters in this book, supramolecular chemistry as well as sample conditions were varied in order to examine whether gel rheological behavior is dependent on factors like polymer functionality sequence, polymer concentration, temperature and pH.

There could be situations where a test material has not been rheologically evaluated. This section focuses on the assessment of an unknown material. As a

Fig. 6 Graph illustrating shear thickening and shear thinning

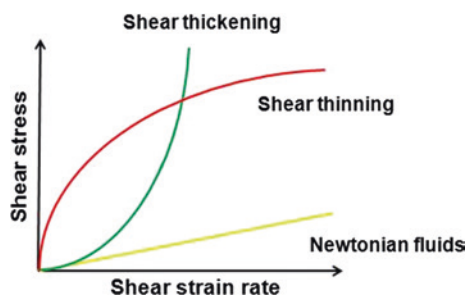
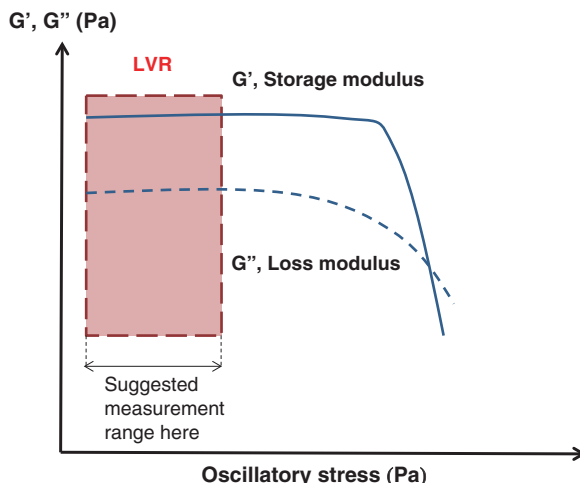


Fig. 7 Graph of an oscillatory stress sweep



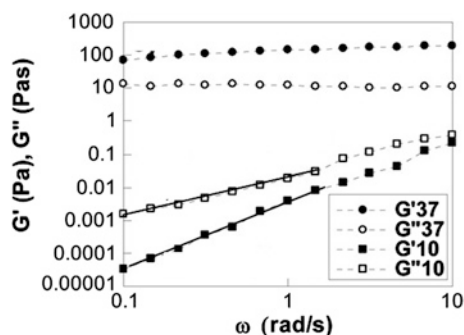
general guide, this section should cover the general rheological characterization of the different unknown materials, however, it also requires certain amount of creativity on the part of the rheologist to design the most appropriate protocol. A point to note is that these recommended conditions could be independently used to further evaluate a materials' rheological response. In all the experiments, it is important that the sample is well conditioned to a particular temperature before proceeding with the measurements.

Most of the time, the rheological properties of a viscoelastic material are strain-independent up to a critical strain level. When the strain exceeds the critical level, the storage modulus of the material declines and a non-linear behavior is observed. The measurement of the strain amplitude dependence of the storage and loss moduli (G' , G'') is a usually the first step taken to characterize a material's viscoelastic behavior and to determine the pseudo-linear viscoelastic region (LVR) of the material. An oscillatory stress sweep (OSS) will give a general range of where the LVR is located. The range of the stress sweep should be tested over the allowable shear stress (torque $\sim 1\text{--}10,000 \mu\text{N m}$) range of the instrument. In future experiments, the shear stress range can be adjusted appropriately to collect only reliable data. As the allowable shear stress range is dependent on the geometry used, torque will be used as the controlled variable. The frequency should be set to a value of about 1 Hz (Fig. 7).

After the material's LVR has been defined by a strain sweep, its structure can be further characterized using a frequency sweep at a strain below the critical strain. This experiment provides more information about the effect of colloidal forces and the interactions among particles.

In a frequency sweep, measurements are made over a range of oscillation frequencies at a constant oscillation amplitude and temperature. Below the critical strain, the elastic modulus G' is often nearly independent of frequency, which is a characteristic of a structured or solid-like material. On the other hand, frequency-dependent elastic modulus is a characteristic of a more fluid-like material.

Fig. 8 Frequency sweep test in the sol (10 °C) and gel (37 °C) phases of the CS-g-(PAF-PEG) polymer aqueous solution (6.0 wt%). Reproduced with permission from [91]



These measurements have been used to determine the sol-gel properties of thermogelling polymers. Jeong et al. studied the sol gel behavior of thermogelling polymers with this approach [91]. The frequency sweep test showed that the sol and gel phases of the PEG-PAF grafted chitosan (CS-g-(PAF-PEG)) aqueous solution were characterized by fluid-like behavior and solid-like behavior (Fig. 8). At 10 °C, the elastic modulus and loss modulus of the aqueous polymer solution were proportional to $\omega^{2.1}$ and $\omega^{1.1}$, respectively, indicating a typical viscoelastic fluid-like phase of the sol [92–94]. In addition, the loss modulus was greater than elastic modulus at 10 °C. At 37 °C, the elastic modulus was greater than the loss modulus by an order of magnitude at 37 °C. The elastic modulus was nearly independent of frequency, whereas the loss modulus slightly decreased as the frequency increased in the investigated frequency range of 0.1–10 rad s⁻¹. In the solution state, the thermogelling system showed viscous fluid-like behavior with $G'' > G'$ and a frequency-dependent modulus, whereas in the gel state, $G' > G''$ and G' was independent of the frequency.

Next, it is important to determine if the material requires pre-treatment (such as pre-shearing) before measurements. This can be determined from the pseudo-viscosity profile of the material. Pre-shearing will determine a zero-time of shear, thereby eliminating any structure history prior to loading. This is done by performing a continuous flow test under the broad torque range. The data can be viewed as viscosity versus torque/stress and converted to viscosity versus shear rate.

Most food formulations, cosmetics, pharmaceuticals and paints are structured fluids, containing droplets of an immiscible fluid or particle suspended in a liquid matrix. The viscosity of the liquid matrix in the dispersions plays an important role on the flow properties of the material. When there are repulsive forces between particles they do not settle rapidly, forming a network structure, which stabilizes the suspension. The delicate network structure can be destroyed by shearing, resulting in decreased fluid viscosity.

Most structured fluids do not obey a simple linear relationship between applied stress and flow (Newtonian fluid behavior). Most of these materials have viscosities, which decrease with increasing stress. Such an observation is known as shear thinning which becomes progressively significant as the volume concentration of solid particles increases.

Another aspect that has to be ascertained is the stability of the material properties over the time of testing. For this experiment, an oscillatory time sweep of about 15 min, with oscillation shear stress/torque within the LVR and a frequency of 1 Hz can be carried out. The material can be pre-sheared at a shear rate beyond the 1st Newtonian plateau determined in the previous step. The experiment is allowed to run and a plot of modulus against time is obtained. The point where the modulus plateaus off is judged to be the minimum time required for the recovery of the material structure. This was applied by Moura et al. to understand the gelation kinetics and gel properties upon crosslinking the hydrogel. Both the components G' and G'' moduli, was monitored. Figure 9 shows the time sweep profiles of elastic (G') and viscous (G'') moduli near the gel point for pure chitosan solution (A) and for 0.10 % (B) and 0.15 % (C) genipin concentration networks. At the beginning, G'' was larger than G' , which was expected because the samples were still in a liquid state and, thus, viscous properties dominated. As the solutions began to turn into a gel-like state due to the formation of the cross-linked network, both moduli increased. However, the rate of increase of G' ($\Delta G'/\Delta t$) was higher than that of G'' because the elastic properties started to dominate. This difference in the rates leads to a G' and G'' crossover. The time required to achieve this crossover is, as mentioned above, the gelation time. From the figure, it is can be seen that higher genipin concentrations lead to lower gelation times. It should also be stressed that the gelation time decreases from about 8 min to about 2 min when the genipin concentration is increased from 0 to 0.15 %.

The creep test probes the time-dependent nature of a sample. Creep and recovery tests allow the differentiation between viscous and elastic responses when the viscoelastic material is subjected to a step constant stress (creep) and then the applied stress is removed (recovery). A standard creep experiment provides critical parameters such as zero shear viscosity (η_0) and equilibrium compliance (J_{eo}), which measures the elastic recoil of a material.

After a sample is allowed to creep under load, the material's elastic behavior can be obtained by abruptly relieving the imposed stress and measuring the extent the sample recovers. A creep/recovery test can be carried out as follows.

- First, standard temperature conditioning and pre-shearing beyond the 1st Newtonian plateau is performed.
- The sample is then equilibrated for a set time necessary to obtain a stable structure as determined earlier in the judgment of the material stability.
- Next, for the retardation step, a shear stress is again selected from within the 1st Newtonian plateau and performed for about 15 min or enough time for slope to be constant.
- Then the recovery of the sample is affected by setting the shear stress to zero and duration for the sample to recover is examined.

During the creep test, the stress causes a transient response, including the elastic and the viscous contributions. By following the recovery phase after the release of the applied stress, one can separate the total strain into the instantaneous elastic part, the recovered elastic part, and the permanently viscous part.

Fig. 9 Dynamics of elastic, G' , and viscous, G'' , moduli near the gel point, at 1 Hz (**a**, pure chitosan; **b** and **c**, 0.10 % (w) and 0.15 % (w) genipin chitosan concentration network, respectively). The gelation time is determined as the time at which G' and G'' intersect each other. Reproduced with permission from [95]

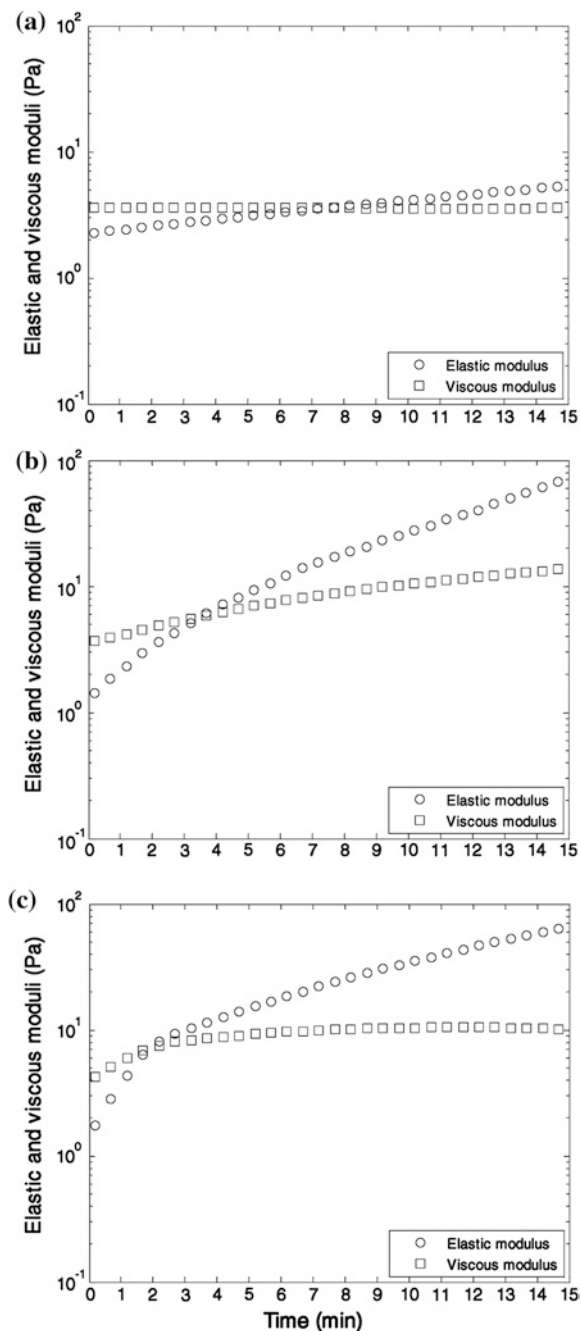
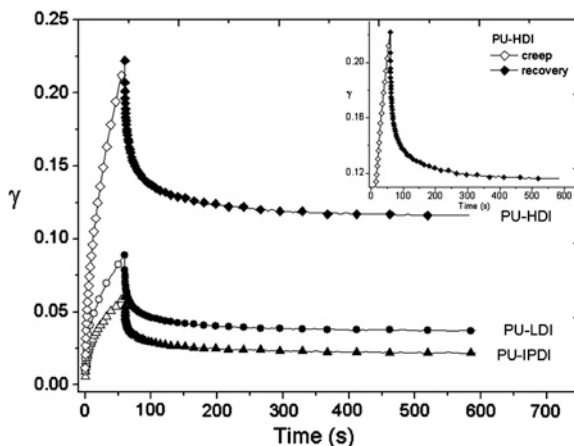


Fig. 10 Creep (*open symbols*) and recovery (*full symbols*) curves for the poly(isopropyl lactate diol)-based polyurethane hydrogels at 37 °C when a stress of 5 Pa was applied for 60 s. Reproduced with permission from [96]



Viscoelastic creep data can be presented by plotting the creep modulus (constant applied stress divided by total strain at a particular time) or the strain, as a function of time. Gradinaru et al. studied the creep response of thermogelling poly(isopropyl lactate diol)-based polyurethane hydrogels [96].

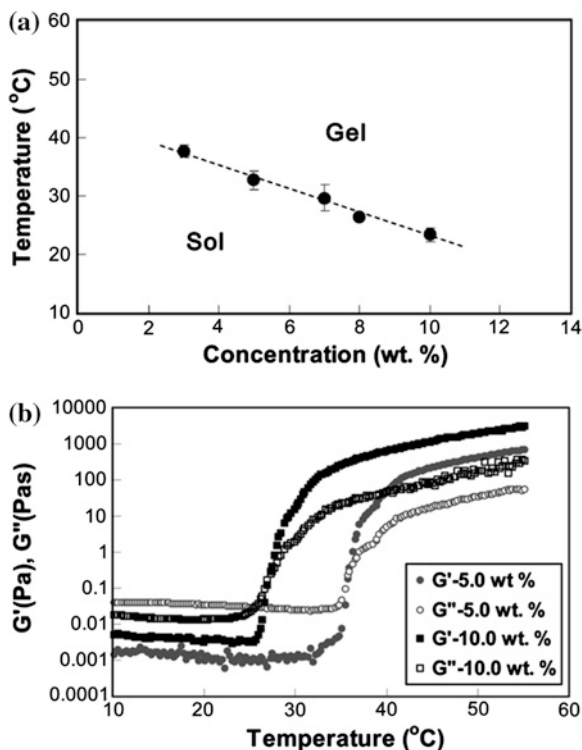
Figure 10 shows the curves that represent the viscoelastic response at an applied stress of 5 Pa for the three hydrogels obtained at 37 °C, in a creep test followed by recovery. The creep curves comprise three parts: the instantaneous strain, the retardation strain, and the viscous strain. When the applied stress is removed, the recovery process starts, and first the instantaneous strain is recovered, then the retardation one, and finally remains the viscous part. The high elasticity of the hydrogels can be observed, where the reached strain after the stress of 5 Pa was applied for 60 s is very high, and the recovered strain represents 52 % from the maximum value reached by the strain in the creep test.

Changes in modulus of thermogelling polymer aqueous solutions can be determined by dynamic rheometry (Fig. 11).

- First, standard temperature conditioning at the lower solution temperature and pre-shearing beyond the 1st Newtonian plateau is performed.
- The sample is then equilibrated for a set time necessary to obtain a stable structure at the lower temperature as determined earlier in the judgment of the material stability.
- Next, the material is subjected to a temperature ramp at a fixed stress and a fixed frequency rate.
- The point at which the elastic and loss modulus intersects is defined as the gel transition temperature.

Jeong et al. reported poly(alanine-co-leucine)-poloxamer-poly(alanine-co-leucine) (PAL-PLX-PAL) aqueous solution [62]. As the temperature increased, the polymer aqueous solution underwent sol-to-gel transition at 20–40 °C in a polymer concentration range of 3.0–10.0 wt%. The sol-gel transition of the polymer aqueous

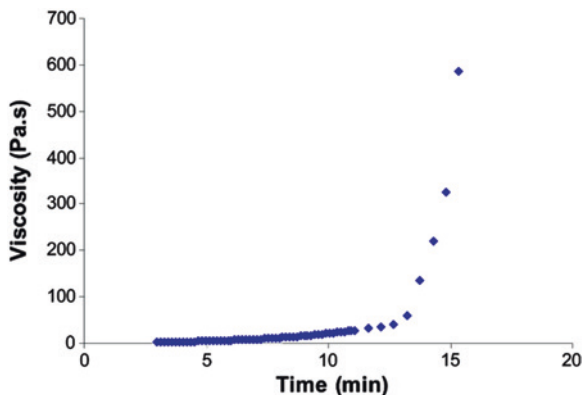
Fig. 11 **a** Phase diagram of the poly(alanine-co-leucine)-poloxamer-poly(alanine-co-leucine) aqueous thermogelling solutions determined by the test tube inverting method. **b** Storage modulus (G') and loss modulus (G'') of the poly(alanine-co-leucine)-poloxamer-poly(alanine-co-leucine) aqueous thermogelling solutions as a function of temperature and concentration. The legends are the concentrations of the polymers in water. Reproduced with permission from [62]



solution was investigated by the test tube inverting method. The aqueous polymer solution (1.0 mL) was put in the test tube with an inner diameter of 11 mm. The transition temperatures were determined by a flow (sol)-no flow (gel) criterion with a temperature increment of 1 °C per step. Each data point is an average of three measurements. Changes in modulus of the polymer aqueous solutions were investigated by dynamic rheometry. The aqueous polymer solution was placed between parallel plates of 25 mm diameter and a gap of 0.5 mm. To minimize the water evaporation during the experiment, the plates were enclosed in a water-saturated chamber. The data were collected under a controlled stress (4.0 dyn/cm²) and a frequency of 1.0 rad s⁻¹. The heating rate was 0.5 °C/min.

The phase diagram of PAL-PLX-PAL aqueous solutions determined by the test tube inverting method is shown in Fig. 11. Aqueous solutions of PAL-PLX-PAL undergo sol-to-gel transition as the temperature increases in a concentration range of 3.0–10.0 wt%. The sol-to-gel transition temperature decreased from 38 to 23 °C as the concentration increased from 3.0 to 10.0 wt%. At concentrations lower than 3.0 wt%, the viscosity of the polymer aqueous solution increased as the temperature increased; however, it was not large enough to resist the flow when the test tube was inverted, and thus they were regarded as a sol state. At polymer concentrations higher than 10.0 wt%, the polymer aqueous system formed a gel in a temperature range of 0–60 °C.

Fig. 12 Variation of viscosity of chitosan-ammonium hydrogen phosphate solution with time as measured using an oscillatory rheometer at a fixed frequency of 1 Hz and fixed temperature of 37 °C. Reproduced with permission from [97]



Sharp increases in both the storage modulus (G') and loss modulus (G'') of PAL-PLX-PAL aqueous solutions were observed as the temperature increased (Fig. 11). G' and G'' are an elastic component and a viscous component of the complex modulus of a system, respectively. When G' is greater than G'' , the system is considered to be a gel, and the crossover point was defined as the sol-to-gel transition temperature. The sol-to-gel transition temperatures defined by the test tube inverting method coincided with those defined by dynamic mechanical analysis of G' and G'' within 2 to 3 °C. By varying the polymer concentration, not only sol-to-gel transition temperature but also modulus of the gel could be controlled. The control of gel modulus (G') has a significant effect on 3D cell culture as well as the differentiation of the stem cell. In the case of chondrocytes, the modulus of 300–2,500 Pa showed a cytocompatible microenvironment for proliferation of the cells. The gel prepared from 10.0 wt% aqueous solution of PAL-PLX-PAL formed a gel with a G' of 380 Pa at 37 °C, thus being recommendable as a 3D culture matrix for chondrocytes.

By raising the temperature above the gelation temperature, the time required for the gelation can be determined. Nair et al. demonstrates the thermogelation of chitosan-ammonium hydrogen phosphate solution determined as a function of time using oscillatory rheometers [97]. The viscosity of the chitosan-ammonium hydrogen phosphate solution was found to increase after 8 min and showed a significant increase within 15 min of incubation at 37 °C, demonstrating the sol-gel transition (Fig. 12).

6 Biomedical Applications

In situ forming hydrogels have been increasingly studied for various biomedical applications such as drug delivery, gene delivery, wound healing, tissue engineering, and microfluidics [83, 98–105]. To use hydrogel systems as drug or gene delivery systems or tissue regeneration matrices, (1) drugs, genes, and/or cells

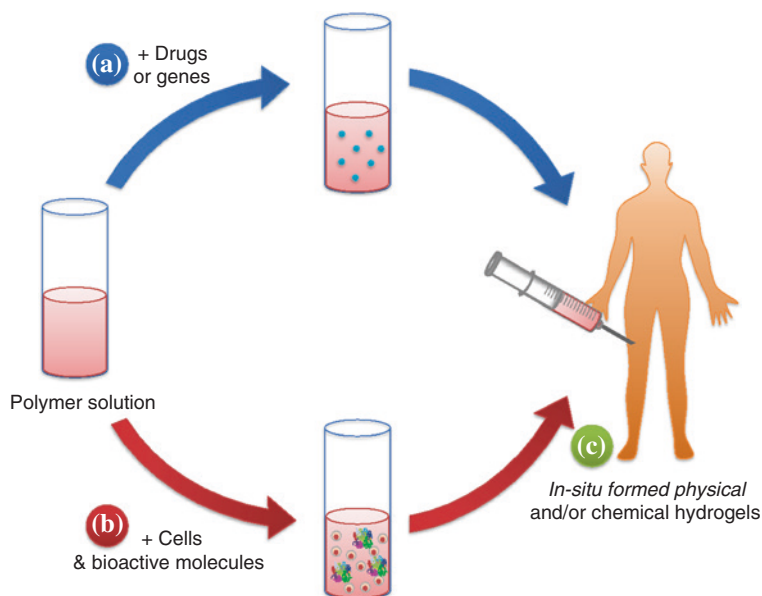


Fig. 13 **a** As injectable drug or gene delivery systems, drugs or genes were dispersed in the polymer solution and then injected to form in situ hydrogel depots. **b** As injectable tissue regeneration matrices, cells and bioactive molecules were mixed with polymer solutions and then injected to the defect area. **c** Injected solutions to the target sites form in situ hydrogels via physical and/or chemical crosslinking

were dispersed in the polymer solution, (2) injected subcutaneously or directly to the defect area, (3) then polymer solutions turn into hydrogels via chemical and/or physical crosslinks (Fig. 13).

“Tetrazole-alkene” photo-click chemistry induced hydrogel of 4-arm PEG-methacrylate (PEG-4-MA) and PEG-4-tetrazole (PEG-4-Tet) showed sustained release of proteins (cytochrome c, γ -globuline, and recombinant human interleukin-2) without losing their bioactivities [37]. PLGA-PEG-PLGA thermosensitive hydrogel with PEG/sucrose and a zinc acetate-exenatide complex (Zn-EXT) showed decreased initial burst and promoted late stage of release of EXT, a glucoregulatory peptide drug for type II diabetes [106]. Nanoscale liposomal polymeric gels (nanolipogels; nLGs) showed sustained delivery of both IL-2 and TGF- β inhibitor and this system enhanced anti-tumor activity against subcutaneous and metastatic melanomas (Fig. 14) [107]. Therapeutic contact lenses of poly[HEMA-co-acrylic acid-co-acrylamide-co-N-vinyl 2-pyrrolidone-co-PEG (200) dimethacrylate] [poly(HEMA-co-AA-co-AM-co-NVP-co-PEG200DMA)] loaded with ketotifen fumarate, a drug that relieves and prevents eye itching, irritation, and discomfort associated with seasonal allergies, showed a dramatic increase in ketotifen mean residence time and bioavailability up to 26 h [108]. A poly(HEMA) based hydrogel containing the ocular drug (DMSA) loaded micelles

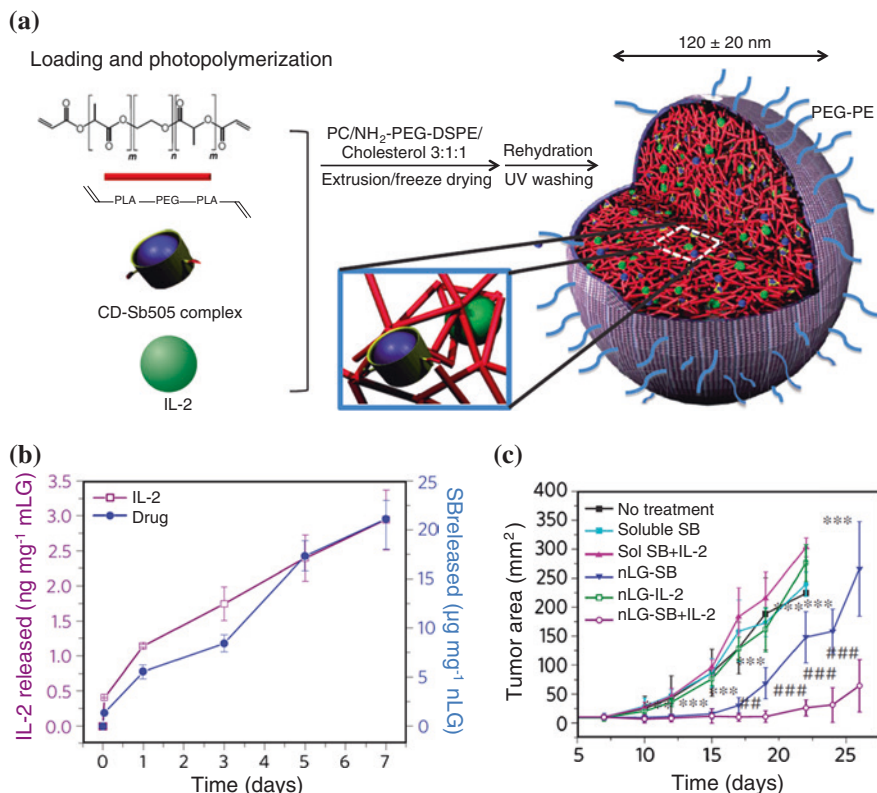


Fig. 14 **a** nLGs were formulated from lyophilized liposomes loaded with biodegradable PLA-PEG-PLA diacrylate, acrylated-CD-TGF- β inhibitor complex, and IL-2 cytokine. After loading, photopolymerization of the polymer and acrylated-CD induced gel formation. **b** Simultaneous release of IL-2 and TGF- β inhibitor released from co-loaded nLGs. **c** Tumor area growth versus time. Reproduced from [107]

(silica shell crosslinked methoxy micelles; SSCMs) was developed as a potential therapeutic contact lens material for long term treatment of ocular disease [109]. In vitro release of DMSA from SSCM embedded hydrogel system was observed over a month. Multiple model drugs of low steric hindrance molecules (LSH) and high steric hindrance molecules (HSH) loaded in the Agarose and Carbomer 974P based hydrogel was suggested as a promising spinal cord injury repair system [110]. LSH released almost completely in 1 day, whereas HSH released only 40 % at day 1 and sustained released during 7 days in vitro. In vivo release was more rapid than in vitro but release pattern was similar with in vitro. LSH can be drugs for short-term neuroprotection purposes, while HSH can be drugs for long-term neuroregeneration approaches. Anticancer drug of Paclitaxel (PTX) loaded PEG-PCL-PEG (PECE) hydrogel showed steady release of PTX for up to 20 days in vitro and prevented recurrence of breast cancer [111]. Another anticancer drug of

Doxorubicin release-profile from the hexamethylene diisocyanate-Pluronic® F127/HA composite hydrogel was almost zero-order release during 28 days [73]. This system also showed antitumor efficacy and therapeutic effects in animal study.

HA and fibrin hydrogels with plasmid DNA (pDNA)/PEI polyplexes loaded through the caged nanoparticle encapsulation were able to deliver genes in vivo without aggregation [112]. Oxidized alginate hydrogels loaded with DNA/PEI nDNA were shown to achieve sustained release in vitro and achieve enhanced revascularization in vivo [113]. Alginate hydrogels conjugated with various RGD densities for siRNA-mediated knockdown of eGFP demonstrated that increasing RGD density resulted in significantly higher knockdown of the targeted protein [114]. Nanostructured micelles-containing PEG based hydrogels that encapsulated cationic bolaamphiphile/DNA complexes and human mesenchymal stem cells (hMSCs) showed higher gene expression efficiency in hMSCs than the PEI/DNA complexes [24]. A CD-based supramolecular hydrogel system with supramolecularly anchored active cationic copolymer/pDNA polyplexes was able to sustain release of pDNA up to 6 days [115]. Hydrogel stiffness can also be used to modulate migration and gene delivery rates; stiffer gels result in slower release rates of encapsulated polyplexes and decreased cell populations, spreading, and transfection [116].

Hydrogels have been used for wound healing as moist wound dressing materials. Hydrogels not only keep the wound moist, but also help proliferation of fibroblasts to recover defects. Rutin-conjugated chitosan-PEG-tyramine hydrogels showed enhanced dermal wound healing efficacy and tissue-adhesive property [117]. Fibroblasts encapsulated PEG-L-PA hydrogels significantly improved in vivo wound healing rate than controls of PBS treated or cell-free PEG-L-PA hydrogel treated group [118]. Treatment of dextran based hydrogels on burn wound promoted neovascularization and skin regeneration [119]. The PECE hydrogel was treated to the full-thickness skin incision wounds and accelerated wound healing compared to untreated controls [111]. In situ forming hydrogels also can be used for prevention of postoperative adhesion [120]. When biodegradable and thermoreversible PCLA-PEG-PCLA hydrogel treated onto the peritoneal wall defect, postoperative adhesion significantly reduced.

In situ hydrogel systems have been used for tissue engineering. For tissue engineering, usually patient-derived healthy cells are expanded in vitro, mixed with polymer solutions and bioactive molecules, and then inject into a defect area to form a hydrogel in situ. Fibronectin- and NT-3-functionalized silk hydrogels that triggered axonal bundling [121] and self-assembling peptide hydrogel of RADA₁₆-IKVAV (AcN-RADARADARADARADAIKVAV-CONH₂) that accelerated central nervous system brain tissue regeneration [122] were developed as neural tissue engineering systems. Thermosensitive PNIPAAm-O-phosphoethanolamine grafted poly(acrylic acid)-PNIPAAm hydrogel showed potential as an osteogenic matrix [123]. Mixture of chondroitin sulfate succinimidyl succinate (CS-NHS) and freeze-thawed bone marrow aspirate formed hydrogels and showed potentials as a meniscus repair system [124] or an articular cartilage regenerative matrix when rhBMP-2 localized within the hydrogel [125]. Thermoresponsive and various

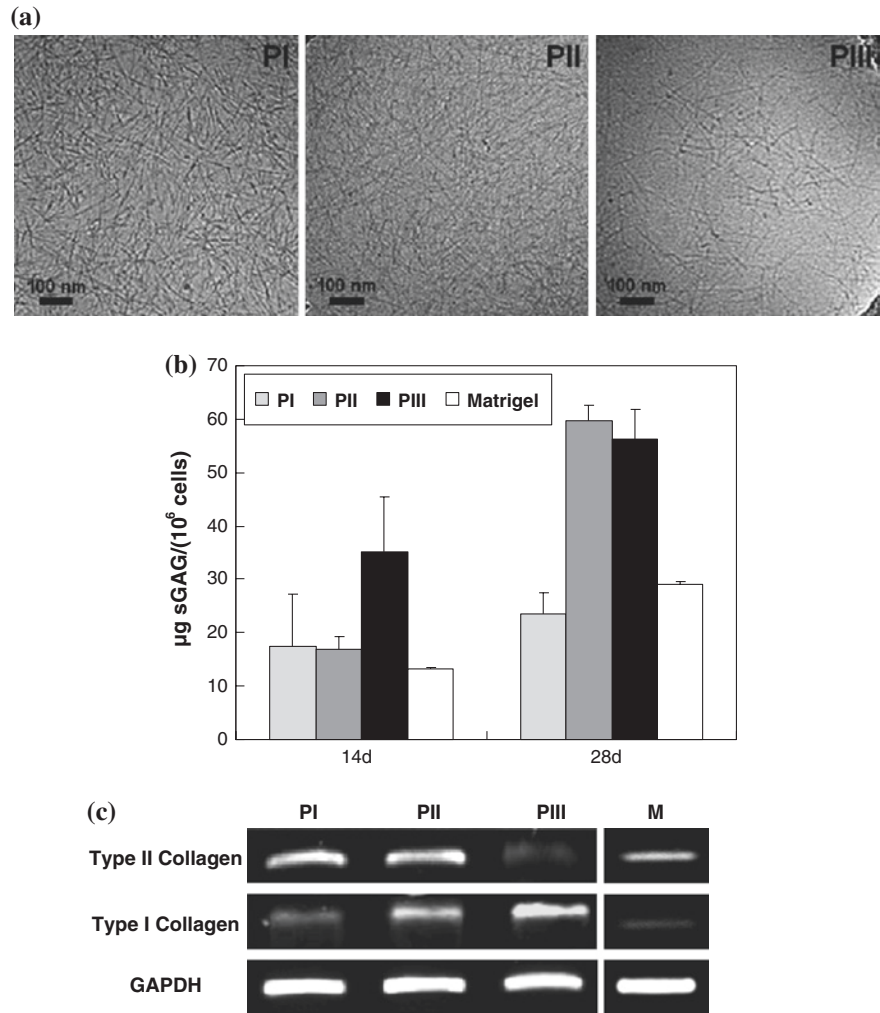


Fig. 15 **a** Nanofibrous interior morphology of (L/DL)-PA-Pluronic[®]-(L/DL)-PA thermogel. Expression of chondrogenic markers of **(b)** sulfated glycosaminoglycan (sGAG) and **(c)** type II collagen. Matrigel[™] was used as a control for 3D chondrocytes culture. Glyceraldehyde 3-phosphate dehydrogenase (GAPDH) is compared as a house-keeping gene. Reproduced from [3]

terminal groups modified PNIPAAm brushes were fabricated for improving cell adhesion and cell sheet harvest [126]. Specifically, carboxyl-terminated PNIPAAm brush surface most enhanced cell adhesion and cell sheet harvesting. (L/DL)-PA-Pluronic[®]-(L/DL)-PA thermogel showed a higher population of nanofibrous structures as the L-Ala content increased and chondrocytes cultured in these thermogels expressed higher chondrogenic markers compared to commercially available Matrigel[™] (Fig. 15) [3].

For the successful tissue regeneration, we need to better understand cell-matrix interactions. Stem cells can be differentiated into specific lineages through the interaction between cell and biological cues or between cell and physical cues [127]. Physicochemical properties of photodegradable PEG based hydrogels could be dynamically controlled by light [9]. Crosslinking density of hydrogel decreased via photodegradation and facilitated spreading or migration of embedded cells. In addition, MSCs showed enhanced chondrogenesis when cell adhesive sequence of Arg-Gly-Asp-Ser (RGDS) was photocleaved from hydrogels. Neurogenesis, myogenesis, and osteogenesis of stem cells on 2D gel surface were controlled by varying stiffness of the hydrogel surface from 0.1–1 kPa, 8–17 kPa, and 25–40 kPa, respectively [128]. Three-dimensional culture of mesenchymal stem cells in RGD-modified alginate hydrogels also showed stem cell differentiation is correlated to the hydrogel stiffness [129]. Briefly, adipogenesis or osteogenesis was predominantly occurred in 2.5–5 kPa or 11–30 kPa microenvironments, respectively. However, cell morphology remained spherical regardless of modulus. MSCs cultured in matrix metalloproteinase (MMP) degradable hydrogels showed high degrees of cell spreading followed by osteogenic differentiation, while remained spherical and underwent adipogenesis in non-degradable hydrogels [14]. MSCs can be induced various differentiation through the interactions between cells and small functional groups in hydrogels [130]. Specifically, phosphate or alkyl groups in PEG hydrogel induced osteogenesis or adipogenesis, respectively. Human adipose derived stem cells (hADSCs) encapsulated in PEG hydrogels with multifunctionalized α -CD nanobeads regulated stem cell fate [131]. Ultimately, the alcohol, hydrophobic methyl group, and phosphate-substituted α -CD nanobeads stimulated chondrogenic, adipogenic, and osteogenic differentiation, respectively.

7 Conclusions and Prospectives

In situ forming chemically and/or physically crosslinked hydrogels under mild conditions have been developed for various biomedical applications. Injectable hydrogel systems are minimally invasive and patient friendly. We can decrease injection frequency for better patient compliance by developing novel sustained drug delivery systems. Cells or bioactive molecules are easy to mix with polymer solutions and these mixtures are in situ and easy to form the 3D microenvironments into any desired defect shapes. For successful designing of an in situ gelling system for a specific biomedical application, several points should be carefully understood. (1) Different crosslinking type gives different degradation products and release-profiles of incorporated drugs. (2) Porosity and pore size of hydrogels can affect to cell viability, proliferation, and/or drug release profile. (3) Initiators, catalysts, or residual monomers can lead cytotoxicity. During radical polymerization, produced radicals not only can react with the vinyl group in monomer but also can damage cellular macromolecules. (4) Reactive functional groups of polymers can give side reactions with incorporated bioactive molecules

or cells. These side reactions might induce immunogenicity and damage cells or the efficacy of drugs. (5) Residual enzyme after enzymatic crosslinking also can provide unexpected reactions with incorporated protein drugs. (6) Development of various hydrogel-based drug delivery systems with non-modified original drug is one of the best ways to produce the improved versions of biologics. Biobetters can advance the efficacy, pharmacokinetic parameters, and safety profile of drugs than original biologics or Biosimilars (subsequent versions of off-patent biologics with demonstrated physicochemical similarity). In addition, Biobetters can also improve patient compliance due to a reduced rate of side effects and enhanced convenience. (7) Sustained-release systems without initial burst release should be considered. The charge interaction or the inclusion complex formation between polymer and drug can improve these problems. (8) Incorporated drugs or cells should be stable during the implantation period. Acidic degradation-products released from polyester-based hydrogels raise the local acidity inside and around the hydrogels, which lead an inflammatory response and a decrease of cell viability or drug stability. (9) For tissue regeneration application, ECM mimicking design of the hydrogel system is a key factor. Polypeptides have unique secondary structures of α -helix, triple helix, β -sheet, or random coil, etc. Different combinations of polypeptide-based hydrogel systems allow various nanostructures in the hydrogels that affect proliferation and/or differentiation of encapsulated cells. (10) Duration of in situ formed hydrogels should be adjusted to match with drug release profile or tissue regeneration rate. (11) Macromers should be selected based on application route. NIPAAm copolymer has been used for “cell sheet” (a tissue-like cellular monolayer) development that already showed successful applications to human clinical studies. However, in vivo application of PNIPAAm hydrogel still has limitation on the toxicity of the residual monomer. (12) Gel modulus, degradability, functional groups can affect stem cell fate. Soft gel improves neurogenesis or adipogenesis, while stiff gel enhances osteogenesis. Degradable or non-degradable hydrogels induces osteogenesis or adipogenesis, respectively. Phosphate groups or alkyl groups can stimulate osteogenesis or adipogenesis, respectively.

Challenging design of hydrogels with these understands and considerations about various hydrogel systems will advance the development of smart bioactive in situ gelling hydrogels for specific biomedical applications.

Also, study of flow properties of liquids is important for pharmacists working in the manufacture of several dosage forms, such as simple liquids, ointments, creams and pastes. The flow behavior of liquids under applied stress is of great relevance in the field of pharmacy. Flow properties are used as important quality control tools to maintain the superiority of the product and reduce batch-to-batch variations.

The clinically approved systems by using Pluronics/alginate (Guardix-SG) and chitosan/glycerol phosphate (BST-CarGel) based thermal gels are interesting examples. Alginate and Pluronics form interpenetrating network (IPN) by adding calcium salt, where it forms a temperature sensitive gelling system. The system was successfully applied as an antiadhesive agent after the surgery. BST-CarGel was applied for articular cartilage repair on the microfractured treatment.

Compared with current microfracture treatment, the BST-CarGel system improved the repair by successfully holding the cells/stem cells released from the microfractured site. Both systems are already on the market. Another system is Regel[®], which was a pioneering system of biodegradable thermogelling system. The biocompatibility was good as evidenced by passing phase I clinical trial. However, the paclitaxel loaded Regel[®] (Oncogel) was stopped for further investigation [132]. When a patient is diagnosed as a solid tumor, he/she immediately wants surgery instead of waiting till the tumor size decreases by using the sustained release of the anticancer drug from the in situ formed gel. Therefore, the treatment was narrowed down for inoperable tumor such as inoperable esophageal cancer. However, compared with current treatment of anticancer drug combined with radiotherapy, the additional treatment by using Oncogel did not significantly improve the patient. Above cases studies suggest that the patient-oriented development of an in situ gelling system is very important.

References

- Berger, J., Reist, M., Mayer, J.M., Felt, O., Peppas, N.A., Gurny, R.: Structure and interactions in covalently and ionically crosslinked chitosan hydrogels for biomedical applications. *Eur. J. Pharm. Biopharm.* **57**, 19–34 (2004)
- Wichterle, O., Lim, D.: Hydrophilic gels for biological use. *Nature* **185**, 117–118 (1960)
- Choi, B.G., Park, M.H., Cho, S.-H., Joo, M.K., Oh, H.J., Kim, E.H., et al.: In situ thermal gelling polypeptide for chondrocytes 3D culture. *Biomaterials* **31**, 9266–9272 (2010)
- Hoffman, A.S.: Hydrogels for biomedical applications. *Adv. Drug Deliv. Rev.* **54**, 3–12 (2002)
- Ko, D.Y., Shinde, U.P., Yeon, B., Jeong, B.: Recent progress of in situ formed gels for biomedical applications. *Prog. Polym. Sci.* **38**, 672–701 (2013)
- Chien, H.W., Tsai, W.B., Jiang, S.Y.: Direct cell encapsulation in biodegradable and functionalizable carboxybetaine hydrogels. *Biomaterials* **33**, 5706–5712 (2012)
- He, X., Ma, J., Jabbari, E.: Effect of grafting RGD and BMP-2 protein-derived peptides to a hydrogel substrate on osteogenic differentiation of marrow stromal cells. *Langmuir* **24**, 12508–12516 (2008)
- Hong, Y., Song, H., Gong, Y., Mao, Z., Gao, C., Shen, J.: Covalently crosslinked chitosan hydrogel: properties of in vitro degradation and chondrocyte encapsulation. *Acta Biomater.* **3**, 23–31 (2007)
- Kloxin, A.M., Kasko, A.M., Salinas, C.N., Anseth, K.S.: Photodegradable hydrogels for dynamic tuning of physical and chemical properties. *Science* **324**, 59–63 (2009)
- Shin, H., Temenoff, J.S., Mikos, A.G.: In vitro cytotoxicity of unsaturated oligo[poly(ethylene glycol) fumarate] macromers and their cross-linked hydrogels. *Biomacromolecules* **4**, 552–560 (2003)
- Temenoff, J.S., Park, H., Jabbari, E., Sheffield, T.L., LeBaron, R.G., Ambrose, C.G., et al.: In vitro osteogenic differentiation of marrow stromal cells encapsulated in biodegradable hydrogels. *J. Biomed. Mater. Res., Part A* **70**, 235–244 (2004)
- Chen, Y.C., Lin, R.Z., Qi, H., Yang, Y., Bae, H., Melero-Martin, J.M., et al.: Functional human vascular network generated in photocrosslinkable gelatin methacrylate hydrogels. *Adv. Funct. Mater.* **22**, 2027–2039 (2012)
- Geng, X.H., Mo, X.M., Fan, L.P., Yin, A.L., Fang, J.: Hierarchically designed injectable hydrogel from oxidized dextran, amino gelatin and 4-arm poly(ethylene glycol)-acrylate for tissue engineering application. *J. Mater. Chem.* **22**, 25130–25139 (2012)

14. Khetan, S., Guvendiren, M., Legant, W.R., Cohen, D.M., Chen, C.S., Burdick, J.A.: Degradation-mediated cellular traction directs stem cell fate in covalently crosslinked three-dimensional hydrogels. *Nat. Mater.* **12**, 458–465 (2013)
15. Fairbanks, B.D., Singh, S.P., Bowman, C.N., Anseth, K.S.: Photodegradable, photoadaptable hydrogels via radical-mediated disulfide fragmentation reaction. *Macromolecules* **44**, 2444–2450 (2011)
16. McCall, J.D., Luoma, J.E., Anseth, K.S.: Covalently tethered transforming growth factor beta in PEG hydrogels promotes chondrogenic differentiation of encapsulated human mesenchymal stem cells. *Drug Deliv. Transl. Res.* **2**, 305–312 (2012)
17. Silva-Correia, J., Zavan, B., Vindigni, V., Silva, T.H., Oliveira, J.M., Abatangelo, G., et al.: Biocompatibility evaluation of ionic- and photo-crosslinked methacrylated gellan gum hydrogels: in vitro and in vivo study. *Adv Healthc Mater.* **2**, 568–575 (2013)
18. Barrow, M., Zhang, H.F.: Aligned porous stimuli-responsive hydrogels via directional freezing and frozen UV initiated polymerization. *Soft Matter* **9**, 2723–2729 (2013)
19. Elisseeff, J., Anseth, K., Sims, D., McIntosh, W., Randolph, M., Langer, R.: Transdermal photopolymerization for minimally invasive implantation. *Proc. Natl. Acad. Sci. U. S. A.* **96**, 3104–3107 (1999)
20. Park, H., Choi, B., Hu, J.L., Lee, M.: Injectable chitosan hyaluronic acid hydrogels for cartilage tissue engineering. *Acta Biomater.* **9**, 4779–4786 (2013)
21. Purcell, B.P., Elser, J.A., Mu, A., Margulies, K.B., Burdick, J.A.: Synergistic effects of SDF-1 α chemokine and hyaluronic acid release from degradable hydrogels on directing bone marrow derived cell homing to the myocardium. *Biomaterials* **33**, 7849–7857 (2012)
22. Shih, H., Lin, C.C.: Visible-light-mediated thiol-ene hydrogelation using eosin-Y as the only photoinitiator. *Macromol. Rapid Commun.* **34**, 269–273 (2013)
23. Lim, K.S., Alves, M.H., Poole-Warren, L.A., Martens, P.J.: Covalent incorporation of non-chemically modified gelatin into degradable PVA-tyramine hydrogels. *Biomaterials* **34**, 7097–7105 (2013)
24. Li, Y., Yang, C., Khan, M., Liu, S., Hedrick, J.L., Yang, Y.Y., et al.: Nanostructured PEG-based hydrogels with tunable physical properties for gene delivery to human mesenchymal stem cells. *Biomaterials* **33**, 6533–6541 (2012)
25. Phelps, E.A., Enemchukwu, N.O., Fiore, V.F., Sy, J.C., Murthy, N., Sulchek, T.A., et al.: Maleimide cross-linked bioactive PEG hydrogel exhibits improved reaction kinetics and cross-linking for cell encapsulation and in situ delivery. *Adv. Mater.* **24**(64–70), 2 (2012)
26. Wang, H., Han, A., Cai, Y., Xie, Y., Zhou, H., Long, J., et al.: Multifunctional biohybrid hydrogels for cell culture and controlled drug release. *Chem. Commun.* **49**, 7448–7450 (2013)
27. Tortora, M., Cavalieri, F., Chiessi, E., Paradossi, G.: Michael-type addition reactions for the in situ formation of poly(vinyl alcohol)-based hydrogels. *Biomacromolecules* **8**, 209–214 (2007)
28. Wang, Z.C., Xu, X.D., Chen, C.S., Yun, L., Song, J.C., Zhang, X.Z., et al.: In situ formation of thermosensitive PNIPAAm-based hydrogels by Michael-type addition reaction. *ACS Appl. Mater. Interfaces* **2**, 1009–1018 (2010)
29. Chawla, K., Yu, T.B., Liao, S.W., Guan, Z.: Biodegradable and biocompatible synthetic saccharide-Peptide hydrogels for three-dimensional stem cell culture. *Biomacromolecules* **12**, 560–567 (2011)
30. Kupal, S.G., Cerroni, B., Ghugare, S.V., Chiessi, E., Paradossi, G.: Biointerface properties of core-shell poly(vinyl alcohol)-hyaluronic acid microgels based on chemoselective chemistry. *Biomacromolecules* **13**, 3592–3601 (2012)
31. Adzima, B.J., Tao, Y., Kloxin, C.J., DeForest, C.A., Anseth, K.S., Bowman, C.N.: Spatial and temporal control of the alkyne-azide cycloaddition by photoinitiated Cu(II) reduction. *Nat. Chem.* **3**, 256–259 (2011)
32. Chen, R.T., Marchesan, S., Evans, R.A., Styan, K.E., Such, G.K., Postma, A., et al.: Photoinitiated alkyne-azide click and radical cross-linking reactions for the patterning of PEG hydrogels. *Biomacromolecules* **13**, 889–895 (2012)

33. van Dijk, M., van Nostrum, C.F., Hennink, W.E., Rijkers, D.T., Liskamp, R.M.: Synthesis and characterization of enzymatically biodegradable PEG and peptide-based hydrogels prepared by click chemistry. *Biomacromolecules* **11**, 1608–1614 (2010)
34. Xu, X.D., Chen, C.S., Lu, B., Wang, Z.C., Cheng, S.X., Zhang, X.Z., et al.: Modular synthesis of thermosensitive P(NIPAAm-co-HEMA)/beta-CD based hydrogels via click chemistry. *Macromol. Rapid Commun.* **30**, 157–164 (2009)
35. Hu, X., Li, D., Zhou, F., Gao, C.: Biological hydrogel synthesized from hyaluronic acid, gelatin and chondroitin sulfate by click chemistry. *Acta Biomater.* **7**, 1618–1626 (2011)
36. Deforest, C.A., Sims, E.A., Anseth, K.S.: Peptide-functionalized click hydrogels with independently tunable mechanics and chemical functionality for 3D cell culture. *Chem. Mater.* **22**, 4783–4790 (2010)
37. Fan, Y., Deng, C., Cheng, R., Meng, F., Zhong, Z.: In situ forming hydrogels via catalyst-free and bioorthogonal “tetrazole-alkene” photo-click chemistry. *Biomacromolecules* **14**, 2814–2821 (2013)
38. Alge, D.L., Azagarsamy, M.A., Donohue, D.F., Anseth, K.S.: Synthetically tractable click hydrogels for three-dimensional cell culture formed using tetrazine-norbornene chemistry. *Biomacromolecules* **14**, 949–953 (2013)
39. Wei, H.-L., Yang, Z., Chu, H.-J., Zhu, J., Li, Z.-C., Cui, J.-S.: Facile preparation of poly(N-isopropylacrylamide)-based hydrogels via aqueous Diels-Alder click reaction. *Polymer* **51**, 1694–1702 (2010)
40. Nimmo, C.M., Owen, S.C., Shoichet, M.S.: Diels-Alder Click cross-linked hyaluronic acid hydrogels for tissue engineering. *Biomacromolecules* **12**, 824–830 (2011)
41. Tan, H.P., Rubin, J.P., Marra, K.G.: Direct Synthesis of Biodegradable Polysaccharide Derivative Hydrogels Through Aqueous Diels-Alder Chemistry. *Macromol. Rapid Commun.* **32**, 905–911 (2011)
42. Menzies, D.J., Cameron, A., Munro, T., Wolvetang, E., Grondahl, L., Cooper-White, J.J.: Tailorable cell culture platforms from enzymatically cross-linked multifunctional poly(ethylene glycol)-based hydrogels. *Biomacromolecules* **14**, 413–423 (2013)
43. Singh, S., Topuz, F., Hahn, K., Albrecht, K., Groll, J.: Embedding of active proteins and living cells in redox-sensitive hydrogels and nanogels through enzymatic cross-linking. *Angewandte Chemie-International Edition* **52**, 3000–3003 (2013)
44. Park, K.M., Lee, Y., Son, J.Y., Oh, D.H., Lee, J.S., Park, K.D.: Synthesis and characterizations of in situ cross-linkable gelatin and 4-arm-PPO-PEO hybrid hydrogels via enzymatic reaction for tissue regenerative medicine. *Biomacromolecules* **13**, 604–611 (2012)
45. Teixeira, L.S.M., Leijten, J.C.H., Wennink, J.W.H., Chatterjea, A.G., Feijen, J., van Blitterswijk, C.A., et al.: The effect of platelet lysate supplementation of a dextran-based hydrogel on cartilage formation. *Biomaterials* **33**, 3651–3661 (2012)
46. Devolder, R., Antoniadou, E., Kong, H.: Enzymatically cross-linked injectable alginate-g-pyrrole hydrogels for neovascularization. *J. Controlled Release* **172**, 30–37 (2013)
47. Davis, N.E., Ding, S., Forster, R.E., Pinkas, D.M., Barron, A.E.: Modular enzymatically crosslinked protein polymer hydrogels for in situ gelation. *Biomaterials* **31**, 7288–7297 (2010)
48. Vermonden, T., Besseling, N.A.M., van Steenberg, M.J., Hennink, W.E.: Rheological studies of thermosensitive triblock copolymer hydrogels. *Langmuir* **22**, 10180–10184 (2006)
49. Jeong, B., Bae, Y.H., Kim, S.W.: Thermoreversible gelation of PEG-PLGA-PEG triblock copolymer aqueous solutions. *Macromolecules* **32**, 7064–7069 (1999)
50. Hwang, M.J., Suh, J.M., Bae, Y.H., Kim, S.W., Jeong, B.: Caprolactonic poloxamer analog: PEG-PCL-PEG. *Biomacromolecules* **6**, 885–890 (2005)
51. Yu, L., Zhang, H., Ding, J.: A subtle end-group effect on macroscopic physical gelation of triblock copolymer aqueous solutions. *Angew. Chem. Int. Ed.* **45**, 2232–2235 (2006)
52. Loh, X.J., Goh, S.H., Li, J.: New biodegradable thermogelling copolymers having very low gelation concentrations. *Biomacromolecules* **8**, 585–593 (2007)

53. Chenite, A., Chaput, C., Wang, D., Combes, C., Buschmann, M.D., Hoemann, C.D., Leroux, J.C., Atkinson, B.L., Binette, F., Selmani, : Novel injectable neutral solutions of chitosan form biodegradable gels in situ. *Biomaterials* **21**, 2155–2161 (2000)
54. Choi, Y.Y., Joo, M.K., Sohn, Y.S., Jeong, B.: Significance of secondary structure in nano-structure formation and thermosensitivity of polypeptide block copolymers. *Soft Matter* **4**, 2383–2387 (2008)
55. Jeong, Y., Joo, M.K., Bahk, K.H., Choi, Y.Y., Kim, H.T., Kim, W.K., Lee, H.J., Sohn, Y.S., Jeong, B.: Enzymatic degradable temperature-sensitive polypeptide as a new in situ gelling biomaterial. *J. Controlled Release* **137**, 25–30 (2009)
56. Kim, S.Y., Kim, H.J., Lee, K.E., Han, S.S., Sohn, Y.S., Jeong, B.: Reverse thermal gelling PEG-PTMC diblock copolymer aqueous solution. *Macromolecules* **40**, 5519–5525 (2007)
57. Lee, B.H., Lee, Y.M., Sohn, Y.S., Song, S.C.: A thermosensitive poly(organophosphazene) gel. *Macromolecules* **35**, 3876–3879 (2002)
58. Liu, C.D., Zhang, Z.X., Liu, K.L., Ni, X.P., Li, J.: Biodegradable thermogelling poly(ester urethane)s consisting of poly(1,4-butylene adipate), poly(ethylene glycol), and poly(propylene glycol). *Soft Matter* **9**, 787–794 (2013)
59. Megged, Z., Haider, M., Li, D., O'Malley Jr, B.W., Cappello, J., Ghandehari, H.: In vitro and in vivo evaluation of recombinant silk-elastinlike hydrogels for cancer gene therapy. *J. Controlled Release* **94**, 433–435 (2004)
60. Sosnik, A., Cohn, D.: Ethoxysilane-capped PEG-PPO-PEO triblocks: a new family of reverse thermo-responsive polymers. *Biomaterials* **25**, 2851–2858 (2004)
61. Wright, E.R., Conticello, V.P.: Self-assembly of block copolymers derived from elastin-mimetic polypeptide sequences. *Adv. Drug Delivery Rev.* **54**, 1057–1073 (2002)
62. Moon, H.J., Choi, B.G., Park, M.H., Joo, M.K., Jeong, B.: Enzymatically degradable thermogelling poly(alanine-co-leucine)-poloxamer-poly(alanine-co-leucine). *Biomacromolecules* **12**, 1234–1242 (2011)
63. Yeon, B., Park, M.H., Moon, H.J., Kim, S.J., Cheon, Y.W., Jeong, B.: 3D culture of adipose-tissue-derived stem cells mainly leads to chondrogenesis in poly(ethylene glycol)-poly(l-alanine) diblock copolymer thermogel. *Biomacromolecules* **14**, 3256–3266 (2013)
64. Kim, W.S., Mooney, D.J., Arany, P.R., Lee, K., Huebsch, N., Kim, J.: Adipose tissue engineering using injectable, oxidized alginate hydrogels. *Tissue Eng., Part A* **18**, 737–743 (2012)
65. Sinthuvanich, C., Haines-Butterick, L.A., Nagy, K.J., Schneider, J.P.: Iterative design of peptide-based hydrogels and the effect of network electrostatics on primary chondrocyte behavior. *Biomaterials* **33**, 7478–7488 (2012)
66. Appel, E.A., del Barrio, J., Loh, X.J., Scherman, O.A.: Supramolecular polymeric hydrogels. *Chem. Soc. Rev.* **41**, 6195–6214 (2012)
67. Lin, N., Dufresne, A.: Supramolecular hydrogels from in situ host-guest inclusion between chemically modified cellulose nanocrystals and cyclodextrin. *Biomacromolecules* **14**, 871–880 (2013)
68. Li, Y., Fukushima, K., Coady, D.J., Engler, A.C., Liu, S., Huang, Y., et al.: Broad-spectrum antimicrobial and biofilm-disrupting hydrogels: stereocomplex-driven supramolecular assemblies. *Angew. Chem. Int. Ed. Engl.* **52**, 674–678 (2013)
69. Buwalda, S.J., Calucci, L., Forte, C., Dijkstra, P.J., Feijen, J.: Stereocomplexed 8-armed poly(ethylene glycol)-poly(lactide) star block copolymer hydrogels: gelation mechanism, mechanical properties and degradation behavior. *Polymer* **53**, 2809–2817 (2012)
70. Miyata, T., Asami, N., Urugami, T.: A reversibly antigen-responsive hydrogel. *Nature* **399**, 766–769 (1999)
71. Ehrbar, M., Schoenmakers, R., Christen, E.H., Fussenegger, M., Weber, W.: Drug-sensing hydrogels for the inducible release of biopharmaceuticals. *Nat. Mater.* **7**, 800–804 (2008)
72. Tan, H.P., Xiao, C., Sun, J.C., Xiong, D.S., Hu, X.H.: Biological self-assembly of injectable hydrogel as cell scaffold via specific nucleobase pairing. *Chem. Commun.* **48**, 10289–10291 (2012)
73. Chen, C., Wang, L., Deng, L., Hu, R., Dong, A.: Performance optimization of injectable chitosan hydrogel by combining physical and chemical triple crosslinking structure. *J. Biomed. Mater. Res., Part A* **101**, 684–693 (2013)

74. Ekenseair, A.K., Boere, K.W., Tzouanas, S.N., Vo, T.N., Kasper, F.K., Mikos, A.G.: Synthesis and characterization of thermally and chemically gelling injectable hydrogels for tissue engineering. *Biomacromolecules* **13**, 1908–1915 (2012)
75. Gil, E.S., Hudson, S.M.: Stimuli-reponsive polymers and their bioconjugates. *Prog. Polym. Sci.* **29**, 1173–1222 (2004)
76. Peppas, N.A., Hilt, J.Z., Khademhosseini, A., Langer, R.: Hydrogels in biology and medicine: From molecular principles to bionanotechnology. *Adv. Mater.* **18**, 1345–1360 (2006)
77. Qiu, Y., Park, K.: Environment-sensitive hydrogels for drug delivery. *Adv. Drug Deliv. Rev.* **53**, 321–339 (2001)
78. Gunn, J.W., Turner, S.D., Mann, B.K.: Adhesive and mechanical properties of hydrogels influence neurite extension. *J. Biomed. Mater. Res., Part A*. **72A**, 91–97 (2005)
79. Discher, D.E., Janmey, P., Wang, Y.L.: Tissue cells feel and respond to the stiffness of their substrate. *Science* **310**, 1139–1143 (2005)
80. Lozoya, O.A., Wauthier, E., Turner, R.A., Barbier, C., Prestwich, G.D., Guilak, F., Superfine, R., Lubkin, S.R., Reid, L.M.: Regulation of hepatic stem/progenitor phenotype by microenvironment stiffness in hydrogel models of the human liver stem cell niche. *Biomaterials* **32**, 7389–7402 (2011)
81. Wang, L.S., Boulaire, J., Chan, P.P.Y., Chung, J.E., Kurisawa, M.: The role of stiffness of gelatin-hydroxyphenylpropionic acid hydrogels formed by enzyme-mediated crosslinking on the differentiation of human mesenchymal stem cell. *Biomaterials* **31**, 8608–8616 (2010)
82. Jeong, B., Kim, S.W., Bae, Y.H.: Thermosensitive sol-gel reversible hydrogels. *Adv. Drug Deliv. Rev.* **64**, 154–162 (2012)
83. Moon, H.J., Ko, D.Y., Park, M.H., Joo, M.K., Jeong, B.: Temperature-responsive compounds as in situ gelling biomedical materials. *Chem. Soc. Rev.* **41**, 4860–4883 (2012)
84. Park, M.H., Joo, M.K., Choi, B.G., Jeong, B.: Biodegradable thermogels. *Acc. Chem. Res.* **45**, 424–433 (2012)
85. Reiner, M., Blair, G.W.S., Hawley, H.B.: The Weissenberg effect in sweetened condensed milk. *J. Soc. Chem. Ind. (London)* **68**, 327–328 (1949)
86. Rivlin, R.S.: Torsion of a rubber cylinder. *J. Appl. Phys.* **18**, 444–449 (1947)
87. Barnes, H.A., Hutton, J.F., Walters, K.: *An Introduction to Rheology*. Elsevier, Amsterdam (1989)
88. Larson, R.G.: The rheology of dilute solutions of flexible polymers: progress and problems. *J. Rheol.* **49**, 1–70 (2005)
89. Mezger, T.G.: *The Rheology Handbook*. Vincentz, Hannover (2006)
90. Miller, D.R., Macosko, C.W.: New derivation of post gel properties of network polymers. *Macromolecules* **9**, 206–211 (1976)
91. Kang, E.Y., Moon, H.J., Joo, M.K., Jeong, B.: Thermogelling chitosan-g-(PAF-PEG) aqueous solution as an injectable scaffold. *Biomacromolecules* **13**, 1750–1757 (2012)
92. Jin, N., Woodcock, J.W., Xue, C., O’Lenick, T.G., Jiang, X., Jin, S., Dadmun, M.D., Zhao, B.: Tuning of thermo-triggered gel-to-sol transition of aqueous solution of multi-responsive diblock copolymer poly(methoxytri(ethylene glycol) acrylate-co-acrylic acid)-b-poly(ethoxydi(ethylene glycol) acrylate). *Macromolecules* **44**, 3556–3566 (2011)
93. Noro, A., Matsushita, Y., Lodge, T.P.: Gelation mechanism of thermoreversible supramacromolecular ion gels via hydrogen bonding. *Macromolecules* **42**, 5802–5810 (2009)
94. O’Lenick, T.G., Jiang, X., Zhao, B.: Thermosensitive aqueous gels with tunable sol gel transition temperatures from thermo- and pH-responsive hydrophilic ABA triblock copolymer. *Langmuir* **26**, 8787–8796 (2010)
95. Moura, M.J., Figueiredo, M.M., Gil, M.H.: Rheological study of genipin cross-linked chitosan hydrogels. *Biomacromolecules* **8**, 3823–3829 (2007)
96. Gradinaru, L.M., Ciobanu, C., Vlad, S., Bercea, M., Popa, M.: Thermoreversible poly(isopropyl lactate diol)-based polyurethane hydrogels: effect of isocyanate on some physical properties. *Ind. Eng. Chem. Res.* **51**, 12344–12354 (2012)
97. Nair, L.S., Starnes, T., Ko, J.W.K., Laurencin, C.T.: Development of injectable thermogelling chitosan-inorganic phosphate solutions for biomedical applications. *Biomacromolecules* **8**, 3779–3785 (2007)

98. Drury, J.L., Mooney, D.J.: Hydrogels for tissue engineering: scaffold design variables and applications. *Biomaterials* **24**, 4337–4351 (2003)
99. Gong, C., Qi, T., Wei, X., Qu, Y., Wu, Q., Luo, F., et al.: Thermosensitive polymeric hydrogels as drug delivery systems. *Curr. Med. Chem.* **20**, 79–94 (2013)
100. Langer, R., Tirrell, D.A.: Designing materials for biology and medicine. *Nature* **428**, 487–492 (2004)
101. Lee, K.Y., Mooney, D.J.: Hydrogels for tissue engineering. *Chem. Rev.* **101**, 1869–1879 (2001)
102. Matricardi, P., Di Meo, C., Coviello, T., Hennink, W.E., Alhaique, F.: Interpenetrating polymer networks polysaccharide hydrogels for drug delivery and tissue engineering. *Adv. Drug Deliv. Rev.* **65**(9), 1172–1187 (2013)
103. Peppas, N.A., Bures, P., Leobandung, W., Ichikawa, H.: Hydrogels in pharmaceutical formulations. *Eur. J. Pharm. Biopharm.* **50**, 27–46 (2000)
104. Vermonden, T., Censi, R., Hennink, W.E.: Hydrogels for protein delivery. *Chem. Rev.* **112**, 2853–2888 (2012)
105. Ziaie, B., Baldi, A., Lei, M., Gu, Y.D., Siegel, R.A.: Hard and soft micromachining for BioMEMS: review of techniques and examples of applications in microfluidics and drug delivery. *Adv. Drug Deliv. Rev.* **56**, 145–172 (2004)
106. Li, K., Yu, L., Liu, X.J., Chen, C., Chen, Q.H., Ding, J.D.: A long-acting formulation of a polypeptide drug exenatide in treatment of diabetes using an injectable block copolymer hydrogel. *Biomaterials* **34**, 2834–2842 (2013)
107. Park, J., Wrzesinski, S.H., Stern, E., Look, M., Criscione, J., Ragheb, R., et al.: Combination delivery of TGF-beta inhibitor and IL-2 by nanoscale liposomal polymeric gels enhances tumour immunotherapy. *Nat. Mater.* **11**, 895–905 (2012)
108. Tieppo, A., White, C.J., Paine, A.C., Voyles, M.L., McBride, M.K., Byrne, M.E.: Sustained in vivo release from imprinted therapeutic contact lenses. *J. Controlled Release* **157**, 391–397 (2012)
109. Lu, C., Yoganathan, R.B., Kociolek, M., Allen, C.: Hydrogel containing silica shell cross-linked micelles for ocular drug delivery. *J. Pharm. Sci.* **102**, 627–637 (2013)
110. Perale, G., Rossi, F., Santoro, M., Peviani, M., Papa, S., Llupi, D., et al.: Multiple drug delivery hydrogel system for spinal cord injury repair strategies. *J. Controlled Release* **159**, 271–280 (2012)
111. Lei, N., Gong, C.Y., Qian, Z.Y., Luo, F., Wang, C., Wang, H.L., et al.: Therapeutic application of injectable thermosensitive hydrogel in preventing local breast cancer recurrence and improving incision wound healing in a mouse model. *Nanoscale* **4**, 5686–5693 (2012)
112. Lei, Y., Rahim, M., Ng, Q., Segura, T.: Hyaluronic acid and fibrin hydrogels with concentrated DNA/PEI polyplexes for local gene delivery. *J. Controlled Release* **153**, 255–261 (2011)
113. Kong, H.J., Kim, E.S., Huang, Y.C., Mooney, D.J.: Design of biodegradable hydrogel for the local and sustained delivery of angiogenic plasmid DNA. *Pharm. Res.* **25**, 1230–1238 (2008)
114. Khormaei, S., Ali, O.A., Chodosh, J., Mooney, D.J.: Optimizing siRNA efficacy through alteration in the target cell-adhesion substrate interaction. *J. Biomed. Mater. Res., Part A* **100A**, 2637–2643 (2012)
115. Li, Z.B., Yin, H., Zhang, Z.X., Liu, K.L., Li, J.: Supramolecular anchoring of dna polyplexes in cyclodextrin-based polypseudorotaxane hydrogels for sustained gene delivery. *Biomacromolecules* **13**, 3162–3172 (2012)
116. Gojini, S., Tokatlian, T., Segura, T.: Utilizing cell-matrix interactions to modulate gene transfer to stem cells inside hyaluronic acid hydrogels. *Mol. Pharm.* **8**, 1582–1591 (2011)
117. Tran, N.Q., Joong, Y.K., Lih, E., Park, K.D.: In situ forming and rutin-releasing chitosan hydrogels as injectable dressings for dermal wound healing. *Biomacromolecules* **12**, 2872–2880 (2011)

118. Yun, E.J., Yon, B., Joo, M.K., Jeong, B.: Cell therapy for skin wound using fibroblast encapsulated poly(ethylene glycol)-poly(l-alanine) thermogel. *Biomacromolecules* **13**, 1106–1111 (2012)
119. Sun, G., Zhang, X., Shen, Y.I., Sebastian, R., Dickinson, L.E., Fox-Talbot, K., et al.: Dextran hydrogel scaffolds enhance angiogenic responses and promote complete skin regeneration during burn wound healing. *Proc. Natl. Acad. Sci. U. S. A.* **108**, 20976–20981 (2011)
120. Zhang, Z., Ni, J., Chen, L., Yu, L., Xu, J.W., Ding, J.D.: Biodegradable and thermoreversible PCLA-PEG-PCLA hydrogel as a barrier for prevention of post-operative adhesion. *Biomaterials* **32**, 4725–4736 (2011)
121. Hopkins, A.M., De Laporte, L., Tortelli, F., Spedden, E., Staii, C., Atherton, T.J., et al.: Silk hydrogels as soft substrates for neural tissue engineering. *Adv. Funct. Mater.* **23**, 5140–5149 (2013)
122. Cheng, T.-Y., Chen, M.-H., Chang, W.-H., Huang, M.-Y., Wang, T.-W.: Neural stem cells encapsulated in a functionalized self-assembling peptide hydrogel for brain tissue engineering. *Biomaterials* **34**, 2005–2016 (2013)
123. Lin, Z., Cao, S., Chen, X., Wu, W., Li, J.: Thermoresponsive hydrogels from phosphorylated aba triblock copolymers: a potential scaffold for bone tissue engineering. *Biomacromolecules* **14**, 2206–2214 (2013)
124. Simson, J.A., Strehin, I.A., Allen, B.W., Elisseeff, J.H.: Bonding and fusion of meniscus fibrocartilage using a novel chondroitin sulfate bone marrow tissue adhesive. *Tissue Eng. Part A* **19**, 1843–1851 (2013)
125. Simson, J.A., Strehin, I.A., Lu, Q., Uy, M.O., Elisseeff, J.H.: An adhesive bone marrow scaffold and bone morphogenetic-2 protein carrier for cartilage tissue engineering. *Biomacromolecules* **14**, 637–643 (2013)
126. Takahashi, H., Matsuzaka, N., Nakayama, M., Kikuchi, A., Yamato, M., Okano, T.: Terminally functionalized thermoresponsive polymer brushes for simultaneously promoting cell adhesion and cell sheet harvest. *Biomacromolecules* **13**, 253–260 (2012)
127. Higuchi, A., Ling, Q.-D., Chang, Y., Hsu, S.-T., Umezawa, A.: Physical cues of biomaterials guide stem cell differentiation fate. *Chem. Rev.* **113**, 3297–3328 (2013)
128. Engler, A.J., Sen, S., Sweeney, H.L., Discher, D.E.: Matrix elasticity directs stem cell lineage specification. *Cell* **126**, 677–689 (2006)
129. Huebsch, N., Arany, P.R., Mao, A.S., Shvartsman, D., Ali, O.A., Bencherif, S.A., et al.: Harnessing traction-mediated manipulation of the cell/matrix interface to control stem-cell fate. *Nat. Mater.* **9**, 518–526 (2010)
130. Benoit, D.S., Schwartz, M.P., Durney, A.R., Anseth, K.S.: Small functional groups for controlled differentiation of hydrogel-encapsulated human mesenchymal stem cells. *Nat. Mater.* **7**, 816–823 (2008)
131. Singh, A., Zhan, J., Ye, Z., Elisseeff, J.H.: Modular multifunctional poly(ethylene glycol) hydrogels for stem cell differentiation. *Adv. Funct. Mater.* **23**, 575–582 (2013)
132. Mckee, S.: Pharma Times, UK News April 7 (2011)

In-Situ Gelling Polymers

For Biomedical Applications

Loh, X.J. (Ed.)

2015, VIII, 226 p. 86 illus., 44 illus. in color., Hardcover

ISBN: 978-981-287-151-0